● Ultra-Low Iridium Anode Catalyst with High Activity and Long-Term Stability for PEM Water Electrolysis

Inorganic Materials Research Laboratory, Functional Material Research Center, TOSOH Corporation
Takuya Okada
Takayoshi Mishima
Ryota Itoine

Proton exchange membrane (PEM) water electrolysis is one of the most promising methods for hydrogen production and a major focus of global research. However, the anode environment in PEM water electrolysis is highly acidic with high potentials due to the oxygen evolution reaction (OER, $2H_2O \rightarrow O_2 + 4H^+ + 4e^-$), necessitating the use of rare and expensive iridium (Ir)-based materials as anode catalysts. In this report, we present a novel anode catalyst that enables a major reduction in Ir usage. We developed Ir-MnO_2, where Ir is incorporated into MnO_2. Ir-MnO_2 is available in two forms: a powder type and an electrode type (with Ir-MnO_2 directly coated onto a porous transport layer), suitable for catalyst-coated membrane and catalyst-coated substrate applications, respectively. In water electrolysis tests using a PEM electrolyzer, Ir-MnO_2 exhibited high activity, achieving current densities exceeding 3 A/cm^2 at 2 V, even with a low Ir loading of 0.05–0.3 mg/cm^2. Furthermore, when Nafion®-N212 (thickness: 50 μm) was used as the PEM, a current density of 4.9 A/cm^2 at 2 V was achieved with an Ir loading of 0.1 mg/cm^2. In addition, during a constant current test at 2 A/cm^2, Ir-MnO_2 operated for 4,000 hours with an average degradation rate of only 6 μV/h at an Ir loading of 0.2 mg/cm^2. The newly developed anode catalyst provides a basis for expanding the practical application of PEM water electrolysis.

1. Introduction

Proton exchange membrane (PEM) water electrolysis is a promising technology for the production of clean hydrogen owing to its high electrolytic efficiency, high current density, low operating temperature (~100 °C), and rapid response [1,2]. A schematic diagram of a typical PEM water electrolyzer is shown in **Fig. 1**. In a PEM water electrolyzer, neutral water is supplied to the anode side, and an external power source is applied for water electrolysis. At the anode, the supplied water is oxidized, resulting in the oxygen evolution reaction (OER, $2H_2O \rightarrow O_2 + 4H^+ + 4e^-$). At the cathode, protons (H^+) generated from the OER migrate through the PEM and are reduced to produce hydrogen via the hydrogen evolution reaction (HER, $2H^+ + 2e^- \rightarrow H_2$). The OER is slow because it is a four-electron, multi-step reaction; thus, it is the rate-determining step in water electrolysis [3]. Therefore, anode catalysts with low OER overpotentials are required for water electrolysis. In addition, the environment in the vicinity of the anode in PEM water electrolysis is highly acidic (pH ~ 2) [4] due to the generation of H^+ from the OER, which severely limits the choice of usable materials. At present, only Ir-

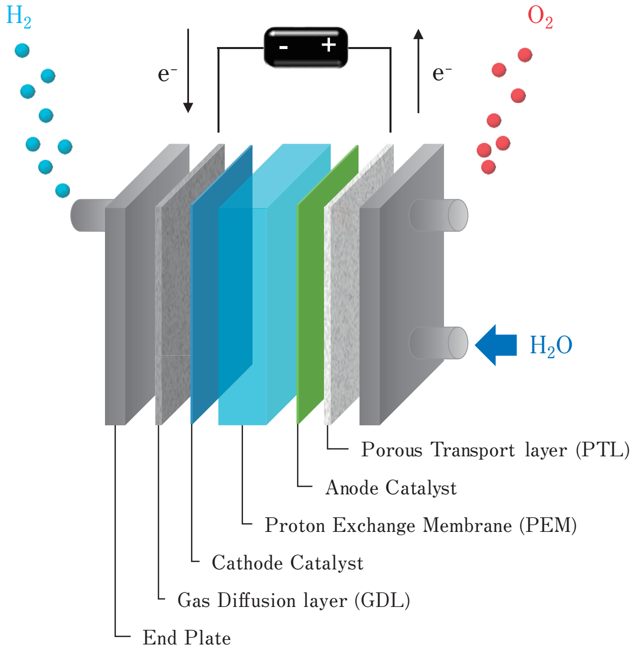

Fig. 1 Schematic diagram of a PEM water electrolyzer

based materials satisfy these requirements [5].

However, Ir is a rare and expensive noble metal, limiting the widespread adoption of PEM water electrolysis technology. The current Ir loading in PEM water electrolyzers is 1–2 mg/cm^2 [1,6]. The annual global production of Ir is only 5–8 tons [7], making it difficult to meet the anticipated hydrogen demand at the 100–1000 GW scale in the future. For example, to manufacture 100 GW of electrolyzers at the current technological level [8], assuming an Ir loading of 2 mg/cm^2 and performance of 3 A/cm^2 at 2 V (corresponding to 0.3 mg$_{Ir}$/W), 30 tons of Ir would be required, clearly indicating that the supply of Ir is severely constrained by resource limitations. In addition, the price of Ir has surged since 2022, reaching $132/g in April 2025 [9], and the current level of Ir usage has a major impact on hydrogen production cost.

Against this background, we aimed to develop a novel anode catalyst with reduced Ir usage. We selected manganese oxides as the base material and developed Ir-MnO_2, incorporating a trace amount of Ir into the MnO_2 structure. In this report, we discuss the applicability of Mn-based materials for PEM water electrolysis and present the characteristics and water electrolysis performance of Ir-MnO_2.

The study aims to support the establishment of clean hydrogen production technologies as a climate action strategy aligned with the SDGs (Goal 7: Affordable and Clean Energy; Goal 9: Industry, Innovation and Infrastructure; and Goal 13: Climate Action).

2. Manganese-Based Catalyst Development

[1] Potential of Manganese-Based Catalysts

Manganese (Mn) is an inexpensive and abundant transition metal capable of exhibiting a wide range of oxidation states (2+, 3+, 4+, and 7+). Owing to these properties, Mn has been extensively studied and applied in various electrochemical devices, such as primary and secondary batteries, supercapacitors, zinc-ion batteries, and electrocatalysts [10–12]. Notably, Mn can stably exist as MnO_2 even under high potentials and strongly acidic

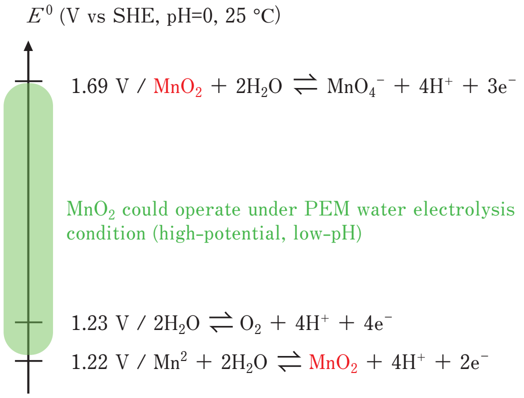

Fig. 2　Standard electrode potentials for each reaction

conditions (**Fig. 2**), which is an unusual property among transition metals. This property suggests that Mn-based materials have the potential to be suitable for the anode environment in PEM water electrolysis.

The application of MnO_2 as an anode material in water electrolysis has been actively investigated by Professor Ryuhei Nakamura's group at the National Institute of Physical and Chemical Research (RIKEN) [13−16].

Typically, MnO_2 is oxidized to soluble MnO_4^- at potentials exceeding 1.69 V vs. SHE (at pH 0) (**Fig. 2**). However, Li et al. (2019) demonstrated that MnO_4^- formation could be suppressed by controlling the anode potential within the stable MnO_2 range in a three-electrode water electrolysis test (pH 2) using γ-MnO_2 as an OER catalyst, thereby achieving stable operation for 8,000 hours [13]. Although manganese oxides are generally known to exhibit low OER activity [10], Kong et al. achieved 2 A/cm^2 at 2 V in a PEM water electrolyzer by increasing the proportion of planar oxygen in γ-MnO_2 [14]. To the best of our knowledge, there are no prior reports of noble-metal-free anode catalysts achieving current densities on the order of 1 A/cm^2 at 2 V in PEM water electrolysis. However, in the same report, a rapid increase in cell voltage was observed after 1,000 hours during a constant current test under the relatively mild condition of 200 mA/cm^2 [14]. Since stable operation for 40,000−80,000 hours is required for PEM water electrolysis [17], substantial improvements in the durability of Mn-based materials are necessary for their practical application as anode catalysts.

[2] Iridium-Reducing Technologies Utilizing Manganese

Recently, Li et al. (2024) reported an OER catalyst for PEM water electrolysis in which Ir is incorporated into MnO_2 [15]. In the reported catalyst, Ir is atomically dispersed on MnO_2 and exists as Ir^{6+} which is known for OER-active species. Typically, Ir^{6+} is a reaction intermediate generated during the OER cycle [18], and there are very few examples where it is stably present in the catalyst. In PEM water electrolysis tests, the reported OER catalyst exhibited exceptionally high activity, achieving 2.3 A/cm^2 at 2 V with an Ir loading of only 0.08 mg/cm^2, and demonstrated stable operation for 3,700 hours at 1 A/cm^2 without performance degradation. It should be noted that a related patent application has been jointly filed by RIKEN and Tosoh Corporation [19].

[3] Tosoh's Manganese Technology

Tosoh has been engaged in the electrolytic manganese dioxide (EMD) business since 1965 and

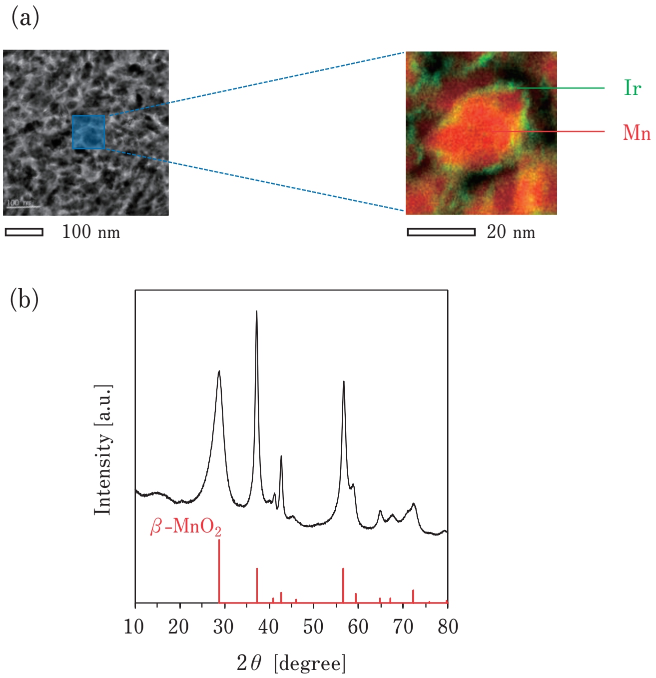

Fig. 3 (a) Cross-sectional TEM image of Ir-MnO_2, (b) XRD patterns of Ir-MnO_2

is the sole supplier in Japan. EMD is produced by the anodic oxidation of Mn^{2+} ions ($Mn^{2+} + 2H_2O \rightarrow MnO_2 + 4H^+ + 2e^-$) through the electrolysis of manganese sulfate ($MnSO_4$) solution. By controlling electrolysis conditions, such as the electrolyte composition and current density, it is possible to flexibly tailor the structural defects and electrochemical potential of EMD [20]. Notably, the Ir-containing MnO_2 reported by Li et al. (2024) was prepared using electrodeposited MnO_2 [15], suggesting a high compatibility with Tosoh's EMD technology.

3. Iridium-Containing Manganese Dioxide (Ir-MnO_2)

[1] Characteristics of the Developed Material

Following the conditions reported by Li et al. (2024) [15], we prepared iridium-containing manganese dioxide (Ir-MnO_2) using our EMD as the base material, followed by detailed characterization and electrochemical tests. We fabricated two forms of Ir-MnO_2.

(i) Electrode-Type Ir-MnO_2

Electrode-type Ir-MnO_2 was prepared by directly fabricating Ir-MnO_2 onto a porous transport layer (PTL), following the methods reported by Li et al. (2024) [15]. The PTL is a component used on the anode side of PEM water electrolyzers (**Fig. 1**), serving to supply electrical power to the catalyst and facilitate mass transport, including water supply and oxygen removal. Typically, the PTL consists of a porous titanium substrate (such as fiber- or powder-sintered structures) coated with platinum. In this study, a Pt-coated titanium sintered fiber (Tanaka Precious Metal Technologies Co., Ltd., Tokyo, Japan) was used as the PTL. Such materials, in which the catalyst and PTL are integrated, are referred to as catalyst-coated substrates (CCS) and can be incorporated directly into water electrolyzers.

(ii) Powder-Type Ir-MnO_2

Powder-type Ir-MnO_2 was prepared following a

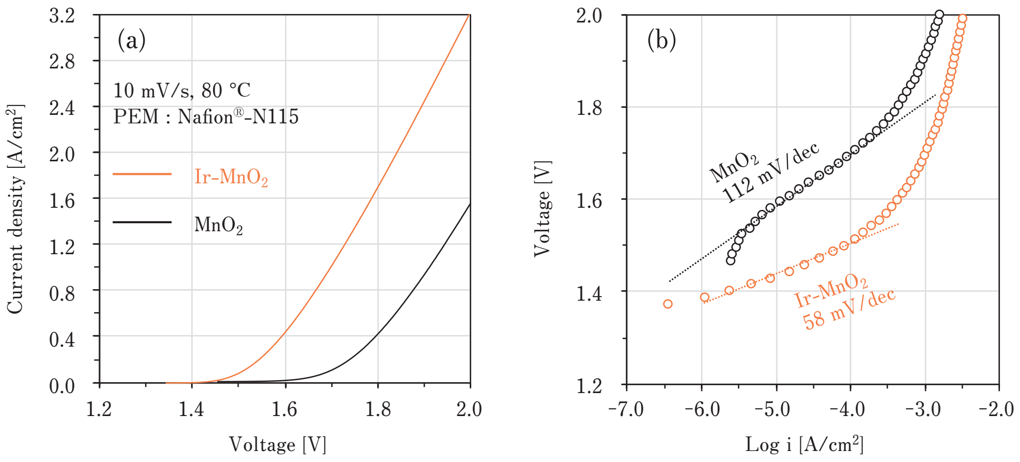

Fig. 4 (a) LSV curves for Ir-MnO$_2$ and MnO$_2$ and (b) corresponding Tafel plots

procedure similar to that used for electrode-type Ir-MnO$_2$. Powder-type Ir-MnO$_2$ can be used to fabricate a catalyst-coated membrane (CCM) by applying a catalyst ink containing Ir-MnO$_2$ onto the PEM. The CCM configuration is commonly used in PEM water electrolysis.

Figure 3a shows the cross-sectional transmission electron microscopy (TEM) image and energy dispersive X-ray spectroscopy (EDS) elemental mapping of electrode-type Ir-MnO$_2$. TEM-EDS mapping revealed that Ir is distributed across the surface of MnO$_2$ crystals with sizes of 20–30 nm. Figure 3b presents the powder X-ray diffraction (XRD) pattern of powder-type Ir-MnO$_2$. All peaks could be assigned to β-type MnO$_2$, and no Ir-related phases were detected. A similar XRD pattern was observed for the electrode-type sample (data not shown). X-ray absorption fine structure (XAFS) measurements were performed on Ir-MnO$_2$ to determine the oxidation state of Ir using the method described by Li et al. (2024) [15]. Consistent with the results of Li et al., the presence of Ir with an average oxidation state higher than 4+ was confirmed. While Ir typically exists in oxidation states ranging from 0+ to 4+ under open-circuit conditions, it is assumed that a portion of Ir in Ir-MnO$_2$ is oxidized by MnO$_2$, resulting in the formation of Ir with a valence state exceeding 4+ (i.e., Ir^{6+}).

［2］Water Electrolysis Performance

The water electrolysis performance of Ir-MnO$_2$ was evaluated using a two-electrode single-cell PEM electrolyzer. Nafion®-N115 (thickness: 127 μm) was used as the PEM, and Pt-supported carbon (Pt: 20 wt%, Pt loading: 0.3 mg/cm^2) was used as the cathode catalyst. Ultrapure water was supplied at a flow rate of 4 mL/min, and the electrolysis temperature was set to 80 °C. All subsequent electrolysis tests were conducted using PEM electrolyzers with the configuration described above. Figure 4 shows the linear sweep voltammetry (LSV) curves (scan rate: 10 mV/s, **Fig. 4**a) and corresponding Tafel plots (**Fig. 4**b) for Ir-MnO$_2$ and MnO$_2$. Both samples were classified as the CCS type, and the MnO$_2$ loading was 2 mg/cm^2. The Ir loading in Ir-MnO$_2$ was 0.1 mg/cm^2 (Ir/Mn molar ratio: 0.02). Ir-MnO$_2$ exhibited much higher activity than that of MnO$_2$, achieving 3.2 A/cm^2 at 2 V. The Tafel slopes for Ir-MnO$_2$ and MnO$_2$ were estimated to be 58 mV/dec and 112 mV/dec, respectively. In general, in the multi-step OER process, the Tafel slope is influenced by the number of electrons transferred before reaching the

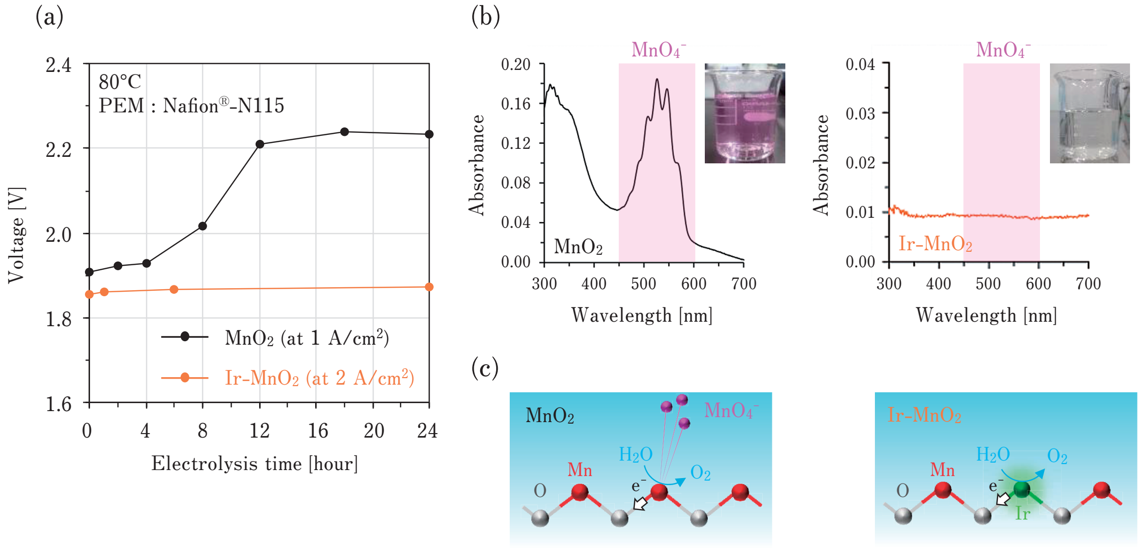

Fig. 5 (a) Voltage profiles at a constant current density for MnO_2 and Ir–MnO_2, (b) UV–vis spectra and photographs of effluents from the electrolyzer for MnO_2 and Ir-MnO_2, and (c) schematic diagrams illustrating OER mechanism for MnO_2 and Ir-MnO_2

rate-determining step. The Tafel slope decreases as the rate-determining step shifts toward the final step of the reaction [21,22]. Therefore, the difference in Tafel slopes observed between Ir-MnO_2 and MnO_2 is considered to be due to a change in the rate-determining step of the OER induced by the introduction of Ir. Tafel slopes of approximately 120 mV/dec are often observed for Mn oxides used as OER catalysts in acidic-to-neutral media [23–25], consistent with the data for MnO_2 in **Fig. 4**b. On the other hand, Tafel slopes of approximately 40–60 mV/dec have been reported for Ir oxides used as OER catalysts in acidic-to-neutral media [22], which is close to that of Ir-MnO_2. These results suggest that Ir acts as the active site for the OER in Ir-MnO_2.

Chronopotentiometry tests for 24 h were conducted at constant current densities of 1 A/cm^2 and 2 A/cm^2 for MnO_2 and Ir-MnO_2, respectively (**Fig. 5**a). For MnO_2, cell voltage increased significantly after 4 hours and reached a plateau at around 2.2 V after 12 hours. A voltage of 2.2 V corresponds to the cell voltage at 1 A/cm^2 without an anode catalyst, indicating total deactivation of the anode catalyst. In contrast, Ir-MnO_2 showed no significant change in cell voltage for at least 24 hours. The entire effluent from the electrolysis of both samples was collected and analyzed through UV-vis spectroscopy (**Fig. 5**b, inset: photographs of the effluents). The effluent from MnO_2 exhibited a pink coloration, and the UV-vis spectrum showed an absorption peak attributable to MnO_4^- [13]. These results indicate that MnO_2 was oxidized to soluble MnO_4^- during the OER ($MnO_2 + 2H_2O \rightarrow MnO_4^- + 4H^+ + 3e^-$). Since MnO_2 itself serves as the active site for the OER, the formation of MnO_4^- directly leads to catalyst loss, increasing cell voltage. As the OER proceeds via adsorption of H_2O on the active site, it is thermodynamically difficult to avoid MnO_4^- formation at high potentials when using MnO_2 as an OER catalyst. In contrast, the effluent from Ir-MnO_2 was colorless, and no absorption peak attributable to MnO_4^- was observed in the UV-vis spectrum. As discussed above, it is reasonable to consider that Ir serves as the active site for the OER in Ir-MnO_2. In other words, it is plausible that MnO_2 does not participate in the OER, thereby suppressing MnO_4^- formation. Schematic illustrations of

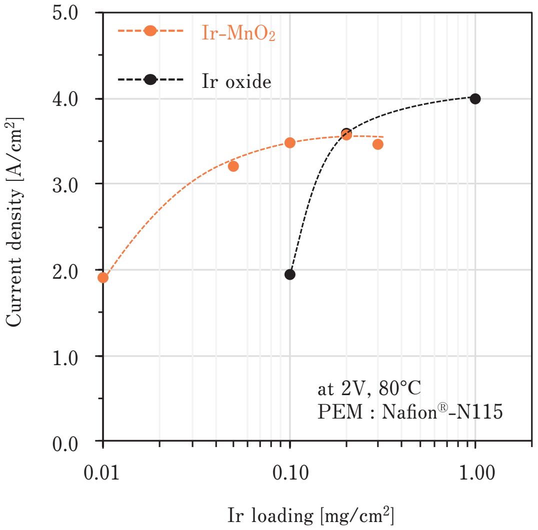

Fig. 6　Current density at 2 V as a function of Ir loading for Ir-MnO_2 and Ir oxide

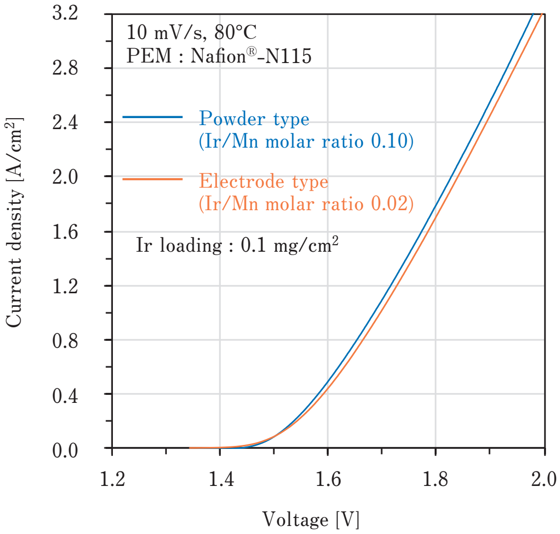

Fig. 7　LSV curves for Ir-MnO_2 in powder and electrode forms

the proposed OER mechanisms for MnO_2 and Ir-MnO_2 are summarized in **Fig. 5**c.

［3］Ir-MnO_2 vs. Iridium Oxide

The water electrolysis performance of Ir-MnO_2 was compared with that of commercial Ir oxide. Figure 6 shows the current density at 2 V as a function of Ir loading for electrode-type Ir-MnO_2 and Ir oxide. For Ir-MnO_2, the MnO_2 loading was fixed at 2 mg/cm^2, and only the Ir loading was varied. For Ir oxide, TEC77100 (Tanaka Precious Metal Technologies Co., Ltd.) was used and evaluated in the CCM configuration. Ir oxide exhibited a significant decrease in current density at Ir loadings below 0.2 mg/cm^2. This could be attributed to reduced electrical contact between catalyst particles on the PEM surface at low Ir loadings, decreasing Ir utilization efficiency. In contrast, Ir-MnO_2 exhibited very high current densities exceeding 3 A/cm^2 even at low Ir loadings (0.05–0.3 mg/cm^2). These findings indicate that the Ir utilization efficiency in Ir-MnO_2 is

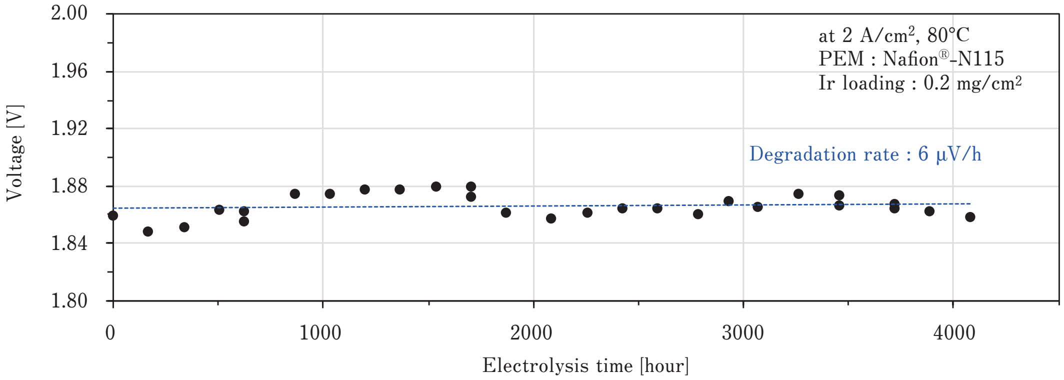

Fig. 8 Voltage profile at constant current density of 2 A/cm² for Ir-MnO_2

higher than that for Ir oxide, suggesting that MnO_2 serves as a conductive pathway ensuring electrical contact for Ir. The Ir consumption per unit power for Ir-MnO_2, calculated from **Fig. 6**, is 0.003–0.04 g_{Ir}/kW, meeting the future reduction target of 0.4 g_{Ir}/kW [26]. Furthermore, even higher current densities can be achieved using a thinner PEM. For example, when Ir-MnO_2 with an Ir loading of 0.1 mg/cm^2 was evaluated using Nafion®-N212 (thickness: 50 μm) as the PEM, a current density of 4.9 A/cm^2 at 2 V was obtained (data not shown).

[4] Effect of Catalyst Configuration (CCM vs. CCS)

As previously described, two types of Ir-MnO_2 were prepared: powder-type and electrode-type. Figure 7 shows the LSV curves for both powder-type and electrode-type Ir-MnO_2. The Ir/Mn molar ratios for the electrode-type and powder-type samples were 0.02 and 0.10, respectively, and the Ir loading was adjusted to 0.1 mg/cm^2 for both. As shown in **Fig. 7**, the water electrolysis activity of Ir-MnO_2 was comparable for the two catalyst configurations. While the preferred configuration (CCM or CCS) may vary depending on the characteristics of the electrolyzer, these results suggest that the configuration of Ir-MnO_2 can be flexibly tailored to meet user requirements.

[5] Durability Test

In PEM water electrolysis, high current densities (above 2 A/cm^2) and long-term operation (5–10 years or 40,000–80,000 h) are required [17]. On the other hand, reducing the Ir content significantly decreases the durability of the anode catalyst, thereby greatly limiting the operational lifetime of the electrolyzer [27,28]. Figure 8 shows the voltage profile of electrode-type Ir-MnO_2 at a constant current density of 2 A/cm^2. The Ir loading was adjusted to 0.2 mg/cm^2 (Ir/Mn molar ratio: 0.02). Despite the low Ir loading of 0.2 mg/cm^2, Ir-MnO_2 operated stably for 4,000 hours with an average degradation rate of only 6 μV/h. This degradation rate is comparable to the target value of 2–5 μV/h set by the U.S. Department of Energy (DOE) [17], indicating that our developed Ir-MnO_2 has the potential for stable long-term operation even at low Ir loadings.

4. Conclusions

Based on EMD manufacturing technology, we developed Ir-MnO_2 by introducing Ir into MnO_2. When applied as an anode catalyst for PEM water electrolysis, Ir-MnO_2 exhibited current densities exceeding 3 A/cm^2 at 2 V and demonstrated stable operation for 4,000 hours at a current density of 2 A/cm^2 with an average degradation rate of only 6 μV/h for an Ir loading as low as 0.1–0.2 mg/cm^2. Ir-MnO_2 is available in both powder and electrode forms, allowing users to select the appropriate catalyst form according to the electrolyzer characteristics. Ongoing Ir-MnO_2 improvements are currently underway to achieve commercialization within the next several years.

Acknowledgments

The authors would like to express their sincere gratitude to Professor Ryuhei Nakamura of RIKEN for his valuable guidance throughout this research. This work includes results obtained from a project commissioned by the New Energy and Industrial Technology Development Organization (NEDO) of Japan (JPNP20003).

References

１）Kara J. Ferner et al., *ACS Appl. Energy Mater.*, **7**, 8124 (2024).
２）Ryan J. et al., Ayers, *ACS Catal.*, **12**, 6159 (2022).
３）Marian Chatenet et al., *Chem. Soc. Rev.*, **51**, 4583 (2022).
４）Marcelo Carmo et al., *Int. J. Hydrogen Energy*, **38**, 4901 (2013).
５）Ahyoun Lim et al., *ACS Catal.*, **15**, 6098 (2025).
６）Sun Seo Jeon et al., *ACS Catal.*, **15**, 4963 (2025).
７）European Commission. https://rmis.jrc.ec.europa.eu/rmp/Iridium
８）Cliffton Ray Wang et al., *Chem. Rev.*, **125**, 1257 (2025).
９）Johnson Matthey https://matthey.com/products-and-markets/pgms-and-circularity/pgm-management
10）Vijay S. Kumbhara et al., Carbon. *Resour. Convers.*, **2**, 242 (2019).
11）Zhaozhao Wang et al., *Electrochem. Commun.*, **151**, 107505 (2023).
12）Masaharu Nakayama et al., *ChemSuSChem*, **18**, e202401907 (2024).
13）Ailong Li et al., Angew. *Chem. Int. Ed.*, **58**, 5054 (2019).
14）Shuang Kong et al., *Nat. Catal.*, **7**, 252 (2024).
15）Ailong Li et al., *Science*, **384**, 666 (2024).
16）Shuang Kong et al., *TOSOH Research & Technology Review*, **65**, 25 (2021).
17）U.S. Department of Energy. https://www.energy.gov/eere/fuelcells/technical-targets-proton-exchange-membrane-electrolysis
18）Raul A. Flores et al., *Chem. Mater.*, **32**, 5854 (2020).
19）WO2022264960A1
20）Kazumasa Suetsugu et al., *TOSOH Research & Technology Review*, **49**, 21 (2005).
21）A. Damjanovic et al., *Electrochim. Acta,* **11**, 791 (1966).
22）Nian-Tzu Suen et al., *Chem. Soc. Rev.*, **46**, 337 (2017).
23）Michael Huynh et al., *J. Am. Chem. Soc.*, **136**, 6002 (2014).
24）Hikaru Abe et al., *ACS Catal.*, **11**, 6390 (2021).
25）Jens Melder et al., *J. Mater. Chem. A*, **7**, 25333 (2019).
26）IRENA Green hydrogen cost reduction, 2020.
27）Haoran Yu et al., *Appl. Catal. B*, **239**, 133 (2018).
28）Fei Wu et al., *Ind. Eng. Chem. Res.*, **61**, 12349 (2022).